

# Characterization of K175 Concrete SNI Standards Using Volcanic Ash Aggregates With Variation in Composition

*by Abd Hakim S*

---

**Submission date:** 03-Oct-2021 04:42AM (UTC-0600)

**Submission ID:** 1663737930

**File name:** Abd\_Hakim\_2020\_J.\_Phys.\_Conf.\_Ser.\_1485\_012064.pdf (1.37M)

**Word count:** 6626

**Character count:** 31850

**PAPER · OPEN ACCESS**

25

## Characterization of K175 Concrete SNI Standards Using Volcanic Ash Aggregates With Variation in Composition

To cite this article: S Abd Hakim *et al* 2020 *J. Phys.: Conf. Ser.* **1485** 012064

17

View the [article online](#) for updates and enhancements.

**IOP ebooks™**

Bringing together innovative digital publishing with leading authors from the global scientific community.

Start exploring the collection—download the first chapter of every title for free.

## Characterization of K175 Concrete SNI Standards Using Volcanic Ash Aggregates With Variation in Composition

Abd Hakim S<sup>1,2</sup>, Kerista Tarigan<sup>2</sup>, Timbangan Sembiring<sup>2</sup>, Manihar Situmorang<sup>3</sup>, Kerista Sebayang<sup>2</sup> and Lia Yulistika Tamba<sup>1</sup>

<sup>1</sup>Department of Physics, Universitas Negeri Medan, Jl. William Iskandar Pasar V, Medan 20211, Indonesia

<sup>2</sup>Department of Physics, Universitas Sumatera Utara, Jl. Bioteknologi No. 1., Medan 20155, Indonesia

<sup>3</sup> Department of Chemistry, Universitas Negeri Medan, Jl. William Iskandar Pasar V, Medan 20211, Indonesia

\*E-mail: abdhakims@unimed.ac.id

**Abstract.** K175 concrete research has been carried out with two types of volcanic ash addition, namely variations of 0%, 6%, 8%, 10%, 12% (K175 concrete) and 15%, 20%, 25%, 30% (density analysis XRD). K175 concrete contributes to residential concrete. The making of K175 concrete refers to SNI 7394: 2008 with compressive strength criteria of 14.53 Mpa. The method used is Precast concrete with sheet pile type. The making of concrete K175 with the addition of cube-shaped volcanic ash with 15 cm sides consisting of cement, sand, broken stone, volcanic ash and water. After casting is done, the concrete is soaked in the tub and then removed from the soaking tub after 28 days of age dried for 24 hours. The following is the water absorption test and compressive strength test by selecting 3 samples which have the optimum compressive strength for XRD, SEM and FTIR tests to see the concrete characterization. Analysis of XRD, SEM, and FTIR are in the variation of 0%, 10% and 25% low absorption, compressive strength respectively 21.06 MPa, 21.16 MPa and 19.46 MPa. The pressure strength also fulfills the compressive strength of Portland cement type I which is 20 MPa.

**Keywords :** Concrete K175, volcanic ash, absorption, compressive strength, analysis (XRD, SEM, FTIR)

### 1. Introduction

Lightweight concrete can be made by injecting air or by removing finer aggregate sizes or by replacing them with hollow, cellular, or porous aggregates. Lightweight concrete density usually ranges from 300 - 1800 kg / m<sup>3</sup> while normal concrete density is around 2,400 kg / m<sup>3</sup>. Lightweight concrete has been categorized into three groups, (1) concrete without fines; (2) lightweight aggregate concrete; and (3) aerated / foamed concrete. Concrete without containing a small amount of aggregate, if any. Coarse aggregate must have a maximum size of 10 mm and 20 mm. The use of mixed



Content from this work may be used under the terms of the Creative Commons Attribution 3.0 licence. Any further distribution of this work must maintain attribution to the author(s) and the title of the work, journal citation and DOI.

aggregates (10 mm and 7 mm; 20 mm and 14 mm) to fill the cavity so that it is distributed evenly is used in reinforced or prestressed concrete construction.

Lightweight aggregate concrete consists of lightweight aggregates (expanded shale material, clay to develop porous structures) which can be used instead of normal aggregates such as broken rock or sand. Foamed concrete is produced using cement paste or mortar [1].

Concrete is a composite mixture formed from cement, aggregate, water, and a mixture or partial cement substitute. The main factors increasing the compressive strength of concrete are using a low water to cement ratio increasing fine fillers, compacting wet concrete and removing cavities. One effective fine filler is silicon dioxide, which is a polymorph of silicon dioxide [2].

High quality concrete is an integral part of many high-rise buildings. In accordance with ACI 211.1-91 the aggregate size of the mixture must be less than 0.5 inches to achieve a compressive strength greater than 9000 psi. On the other hand the distribution of aggregates suitable for the design of concrete mixes is a big problem, the authors propose the proportion of mixtures using additional aggregates of volcanic ash instead of ultra-fine concrete aggregates (concrete silica sand powder).

Portland cement consists of two thirds of mass, calcium silicate ( $3\text{CaO} \cdot \text{SiO}_2$  and  $2\text{CaO} \cdot \text{SiO}_2$  (in cement notation  $C = \text{CaO}$ ,  $S = \text{SiO}_2$ ; respectively C3S and C2S)) one third of aluminum- ( $3\text{CaO} \cdot \text{Al}_2\text{O}_3$  or C3A) and iron- ( $4\text{CaO} \cdot \text{Al}_2\text{O}_3 \cdot \text{Fe}_2\text{O}_3$  or C4AF) containing phases and other crystalline compounds [3]. During the hydration process, water reacts with cement particles (called clinkers) and some chemical and physical reactions take place. cement has capillary pores called macropores or mesoporous caused by empty space after the hydration reaction takes place. Hydrated cement structures are very complex and consist of pores of different sizes where water molecules can be found.

The degree of crystallinity and purity were analyzed using x-ray diffraction (XRD), and analysis of higher resolution of texture and the presence of impurities using electron microscopy x-ray spectroscopy with dispersive energy (SEM-EDS), the functional groups of the samples were analyzed by FTIR.

Mix the proportion of concrete in  $\text{kg} / \text{m}^3$ , made of cement, ordinary sand, gravel (broken stone) and volcanic ash (AV), volcanic ash is similar to the size of fine rubber particles [4]. Deformation of normal aggregate concrete specimens is more symmetrical when crushed. Normal aggregate concrete specimens and Mount Sinabung volcanic ash concrete specimens are the analyzes in this study. Very small volcanic ash particles have sizes smaller than  $1 \mu\text{m}$ . Silica sand powder concrete aggregate size maximum less than  $150 \mu\text{m}$  [2], with a 20 MPa compressive test is 1) using a low water ratio for high grade cement, 2) Suitable pozzolanic material can be added to the mixture design, 3) High-performance concrete can be achieved using sufficient super-plasticizers, 4) Chemical processes can be improved by heat treatment. Material which has pozzolanic properties, such as fly ash, slag, and as an additional cement material which is useful to increase mechanical properties and durability [5]. Total  $\text{SiO}_2 + \text{Al}_2\text{O}_3 + \text{Fe}_2\text{O}_3 > 70\%$  indicates it can be used as a pozzolanic material (ASTM C-618) [6].

The use of large amounts of cement requires a high  $w / c$  ratio, but the shrinkage ratio of the concrete must be reduced because it plays a very important role 1) reduction in interface tension, 2) Release of water trapped between cement particles, 3) Slowing effect of cement hydration, 4) Changing the morphology of hydrated semen.

The process of making concrete quality k175 uses a ratio of 326 kg of cement, 760 kg of sand, 1029 kg of gravel and 215 liters of water. If you want to make this type of concrete tailored to your needs, then you can use a 1: 2: 3 rough dose between cement, sand and gravel, see table 1 (SNI 7394: 2008) supported by table 1.2 [7] in contrast to table 1.3 [8].

Based on table 1.1, the K175 concrete composition has a size of 3: 4: 5: 6 or 6%, 8%, 10% and 12% of the total weight of cement used for normal aggregate concrete specimens while the Mount Sinabung volcanic ash concrete specimens are based on analysis of density XRD used is 15%, 20%, 25% and 30% of the total weight of sand used. This study uses the method of absorption, compressive strength, XRD, SEM, and FTIR.

**TABLE 1.1** Composition of Reference Concrete with Aggregates (SNI 7394: 2008).

Name of material	Mass/Volume		comparison
	(Kg/m <sup>3</sup> )	(Kg/ cm <sup>3</sup> )	
cement	326	0,326	1
sand	760	0,760	2,3
Broken stone	1029	1,029	3,2
water	215	0,215	0,66
Total	2330	2,33	7,16

Cement replacement material has the property of pozzolanic material which can improve concrete characteristics. [9], the test samples composition of 25%, 30%, and 35% of ceramic tile waste showed sufficient strength while the sample composition of 40% of ceramic tile waste showed good. Portland cement is usually filled with fine fillers weighing 10%, 20%, 40% and 60% to form four types of concrete CB-10, CB-20, CB-40, and CB-60. The proportion of concrete mixes in building construction is cement: fine aggregate: coarse aggregate = 1: 2: 4 used, water / cement ratio of 0.6 to 28-day cylinder compressive strength [8]; [10] as reference concrete / control. The concrete mixture increases slightly with the addition of fine aggregate as a substitute for a portion of sand.

**Table 1.2** Composition of the Control Concrete [7].

	Volume (L/m <sup>3</sup> )	Mass (kg/m <sup>3</sup> )
Cement	114.8	350.0
Fine aggregates (mm)		
0 - 0.063	0.0	0.0
0.063 - 0.125	16.0	42.0
0.125 - 0.25	43.6	114.1
0.25 - 0.5	50.0	131.1
0.5 - 1	57.5	150.6
1 - 2	66.0	173.0
Coarse aggregates (mm)		
2 - 4	75.8	198.7
4 - 5.6	40.8	106.9
5.6 - 8	46.3	121.4
8 - 11.2	46.9	122.7
11.2 - 16	120.8	316.5
16 - 22.4	122.1	320.0
Water	182.0	182.0
Voids	17.4	—
Total	1,000	2,329.0

**Table 1.3** Composition of Original Concrete [8].

Komposisi	wt%
CEM II 42.5R	7,9
Sand	23,1
Fly ash	4,8
Coarse aggregate	58,8
Plasticizer	0,1
Water	5,3

The mixing approach is to make concrete strong and durable [11] ie coarse aggregate mixed with additive applications and the amount of water needed for the coating, adding cement with fine aggregate, and mixing the final concrete with the remaining water and plasticizer.

**Tabel 1.4** Komposisi CEM IV / B (P) 32,5 R dan PÇ-42,5 tipe Portland Cement [12].

% OXIDE	% OXIDE	% OXIDE	% OXIDE	% OXIDE	% OXIDE
Al <sub>2</sub> O <sub>3</sub> : 20.178	Cr <sub>2</sub> O <sub>3</sub> : 0.010	K <sub>2</sub> O: 2.545	NiO: 0.005	SiO <sub>2</sub> : 63.352	ZnO: 0.116
BaO: 0.034	CuO: 0.015	MgO: 3.253	P <sub>2</sub> O <sub>5</sub> : 0.200	SrO: 0.015	ZrO <sub>2</sub> : 0.011
CaO: 3.653	Fe <sub>2</sub> O <sub>3</sub> : 3.025	MnO <sub>2</sub> : 0.088	Rb: 0.003	TiO <sub>2</sub> : 0.443	-
Cl: 0.009	Ga <sub>2</sub> O <sub>3</sub> : 0.001	Na <sub>2</sub> O: 2.996	SO <sub>3</sub> : 0.047	Y <sub>2</sub> O <sub>3</sub> : 0.001	-

Cement mortar production is CEM IV / B (P) 32.5 R type pozzolanic pement and PÇ-42.5 type portland cement [12] the composition can be seen in table 1.4 Mortar residue attached to recycled concrete aggregates always leads on decreasing Young's modulus and increasing shrinkage of concrete drying, mainly due to an increase in total mortar volume.

## 2. MATERIALS AND METHODS

### 2.1 Materials and Mix Design

The material used in this study can be seen in Figure 2.1 consisting of cement, fine aggregate (river sand, volcanic ash), coarse aggregate (broken rock) and water. The cement used in this research is PORTLAND CEMENT TYPE I (Ordinary Portland Cement) according to SNI 2049: 2015 ASTM C 150 / C 150M-12BS EN 197-1: 2000 Cement. Volcanic ash comes from Mt. Sinabung. Volcanic ash is designed for two species, namely concrete sp. K175 coded A<sub>0</sub>, A<sub>6</sub>, A<sub>8</sub>, A<sub>10</sub> and A<sub>12</sub> sieved at 120 mesh size, density analysis species with XRD coded B<sub>15</sub>, B<sub>20</sub>, B<sub>25</sub>, and B<sub>30</sub> were not sieved. Each sample code is made in 3 experiments such as A<sub>0-I</sub>, A<sub>0-II</sub> and A<sub>0-III</sub> and so on A<sub>6-I</sub>, A<sub>6-II</sub> and A<sub>6-III</sub>, A<sub>8-I</sub>, A<sub>8-II</sub> and A<sub>8-III</sub>, A<sub>10-I</sub>, A<sub>10-II</sub> and A<sub>10-III</sub>, A<sub>12-I</sub>, A<sub>12-II</sub> and A<sub>12-III</sub>, B<sub>15-I</sub>, B<sub>15-II</sub> and B<sub>15-III</sub>, B<sub>20-I</sub>, B<sub>20-II</sub> and B<sub>20-III</sub>, B<sub>25-I</sub>, B<sub>25-II</sub> and B<sub>25-III</sub>, B<sub>30-I</sub>, B<sub>30-II</sub> and B<sub>30-III</sub>. For the purpose of characterizing the XRD test, the SEM test and the FTIR test were selected for the optimal specifications of the absorption test and the compressive strength test.



**FIGURE 2.1** Material used a) water, b) Portland cement type I, c) broken stone, d) sand, e) volcanic ash

The design was made according to table 1 (SNI 7394: 2008) of normal concrete K175 by reducing the composition of cement and adding volcanic ash can be seen in table 2.1, while the K175 concrete analysis of density XRD according to table 1 by reducing sand adding volcanic ash can be seen in Table 2.2.

**Table 2.1** Concrete quality of K175 by reducing cement adds sifted volcanic ash to 120 mesh.

Concrete	Cement G /cm <sup>3</sup>	Sand G /cm <sup>3</sup>	Broken Stone G /cm <sup>3</sup>	Volcanic Ash G /cm <sup>3</sup>	Water G /cm <sup>3</sup>
A <sub>0</sub>	1,3176	3,0312	4,2168	-	0,7248
A <sub>6</sub>	1,2385	3,0312	4,2168	0,0790	0,7248
A <sub>8</sub>	1,2122	3,0312	4,2168	0,1050	0,7248
A <sub>10</sub>	1,1858	3,0312	4,2168	0,1318	0,7248
A <sub>12</sub>	1,1595	3,0312	4,2168	0,1581	0,7248

**Table 2.2** Concrete quality K175 density analysis of XRD by reducing sand adding unsaved volcanic ash.

Concrete	Cement G /cm <sup>3</sup>	Sand G /cm <sup>3</sup>	Broken Stone G /cm <sup>3</sup>	Volcanic Ash G /cm <sup>3</sup>	Water G /cm <sup>3</sup>
B <sub>15</sub>	1,3176	2,5765	4,2168	0,4546	0,7248
B <sub>20</sub>	1,3176	2,4249	4,2168	0,6062	0,7248
B <sub>25</sub>	1,3176	2,2734	4,2168	0,7578	0,7248
B <sub>30</sub>	1,3176	2,1218	4,2168	0,9092	0,7248

## 2.2 Specimen Preparation

Based on the above composition which has been given code A<sub>0</sub>, A<sub>6</sub>, A<sub>8</sub>, A<sub>10</sub> and A<sub>12</sub>; B<sub>15</sub>, B<sub>20</sub>, B<sub>25</sub>, and B<sub>30</sub> are labeled on each print. Each material is mixed using Molen according to Tables 2.1 and Table 2.2, first sand and cement are mixed evenly, then aggregate (fine / coarse) and water according to the code. The mass of the wet concrete as  $m_1$  is weighed when inserted is molded, after 24 hours the dried concrete is weighed again as the mass of concrete  $m_2$  to determine the absorption of concrete using equation 1. The effective porosity of the specimen is calculated based on the mass variation of the specimen after being immersed in water and dried with air for 24 hours [13] equation (1) in this study was not done only by SEM-EDX characterization.

$$P = \left[ 1 - \left( \frac{m_2 - m_1}{\rho_w v} \right) \right] \times 100 \% \quad (1)$$



**FIGURE 2.2** Tools used a) 120 mesh sieve, b) scales, c) molen, d) compressive strength test equipment, e) XRD, f) SEM\_EDX, g) FTIR.

where P is porosity (%),  $m_1$  is the mass of the test specimen in water (g),  $m_2$  is the mass of the test specimen after 24 hours of air drying (g), v stands for the volume of the test specimen ( $\text{cm}^3$ ), and  $\rho_w$  is the density of water at room temperature ( $\text{g} / \text{cm}^3$ ). Concrete absorption according to [14] in equation (2) in the age of concrete 7 days, 28 days etc of 24 hours the formation of concrete:

$$\text{Absorption} = \left( \frac{m_b - m_k}{m_k} \right) \times 100 \quad (2)$$

where:  $m_b$  = mass of wet concrete (kg)  $m_k$  = mass of dry concrete (kg).

Then the K175 quality concrete is dried at room temperature for 28 days in normal concrete  $A_0$ , then the mountain fly ash concrete that has been sifted  $A_6$ ,  $A_8$ ,  $A_{10}$  and  $A_{12}$  and the mountain fly ash concrete that is not sifted  $B_{15}$ ,  $B_{20}$ ,  $B_{25}$ , and  $B_{30}$  based (analysis density) with XRD compressive strength test. After analyzing the three best samples obtained, namely  $A_{0-III}$ ,  $A_{10-III}$  and  $B_{25-II}$  which were characterized using XRD, SEM-EDX and FTIR.

### 2.3 Testing Methods

Measuring concrete with a ratio of cement: sand: split stone / gravel 1: 2: 3 volume of cement has a 1/6 part of  $1 \text{ m}^3$  concrete =  $0.167 \text{ m}^3$ , Sand has a 2/6 part of  $1 \text{ m}^3$  concrete =  $0.333 \text{ m}^3$ , Split Stone / Gravel has a 3/6 part of  $1 \text{ m}^3$  concrete =  $0.5 \text{ m}^3$ . Planning concrete tests (concrete cubes) has a size of  $15 \times 15 \text{ cm}^2$ , then the volume of concrete cubes that will be made with a thickness of 15 cm is  $0.15 \times 0.15 \times 0.15 \text{ m}^3 = 0.003375 \text{ m}^3 = 3375 \text{ cm}^3$ . Concrete made according to the rules set by SNI (Indonesian National Standard) K175 quality concrete means that it has a compressive strength of 175  $\text{kg} / \text{cm}^2$  issued by the Public Works Agency by (1) reducing cement adding volcanic ash sifted to table 2.1 [2], (2) reducing sand adding volcanic ash not sifted Table 2.2 [1].

## 3. Results and Discussion

The making of volcanic ash concrete has been successfully made with the following materials: cement, fine aggregate (ordinary sand and volcanic ash), coarse aggregate (broken rock) and water. The specimens were removed after 28 days from the soaking bath and placed in the treatment room until the samples dried for 24 hours. Then a mechanical test is carried out, namely water absorption, compressive strength, XRD test, SEM test and FTIR test. The compressive strength of concrete is very much determined by the composition of the material, which is the ratio between gravel, cement, ordinary sand, volcanic ash and water. In this study the manufacture of quality concrete K175 with a composition namely: cement: fine aggregate: coarse aggregate = 1: 2: 3. To determine the characteristics of the concrete needs to be tested namely water absorption, compressive strength, XRD test, SEM test and FTIR test, below can be seen the results of testing of samples.

### 3.1 Testing Methods

Water absorption in concrete can increase at 7 days or decrease at 28 days [14], water absorption provides information about the porosity of concrete studied at ages 7 and 28 days. Water absorption test to determine the ability of concrete to absorb water is made and maintained for 28 days after drying for 24 hours. Determination of water absorption in concrete can be obtained from the measurement of dry mass and wet mass. The results of water absorption from concrete with the addition of volcanic ash can be seen in the Figure 3.1.

Water absorption in a concrete is influenced by pores or cavities. The more pores contained in the concrete, the greater the absorption so that the resistance will be reduced. From the graph above the smallest absorption capacity in normal concrete is 0.3343 and the high water absorption is at the addition of volcanic ash 10% of the cement mass of 0.443, while the addition of 25% volcanic ash as a substitute for sand has an absorption of 0.3399. From the graph above it can be concluded that the size of the absorption is determined by the composition and size of volcanic ash aggregates.



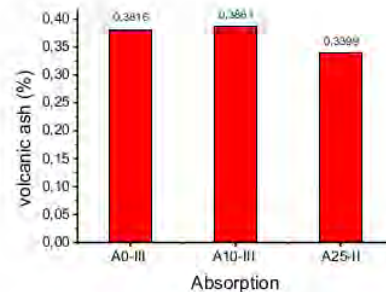


**FIGURE 3.1** Graph of water absorption in concrete from variations of volcanic ash (original)

Porosity is increasing but compressive strength decreases, compressive strength of porous concrete water is usually determined by friction of rough aggregate occlusion and bond strength between aggregate and cement mortar [15], the results of research have used this Mount Sinabung volcanic ash filler as a 10% aggregate (A<sub>10-III</sub>) volcanic ash is sieved, 25% (B<sub>25-II</sub>) volcanic ash is not sifted, clearly differentiating fine and coarse aggregates, while A<sub>0-III</sub> without volcanic ash. The porosity associated with the pores of concrete can be seen morphologically from SEM sequentially getting smaller are A<sub>10-III</sub>, A<sub>0-III</sub>, and B<sub>25-II</sub> in Figure 3.4.

### 3.2 Analysis of Compressive Strength Testing

Coarse aggregate acts as a concrete framework that can determine the properties of a concrete mixture, mechanical properties and durability after hardening [15]. Concrete compressive strength testing is carried out after 28 days after casting and soaking. Water absorption has the most important effect on aggregate characteristics, further affecting the compressive strength [16].

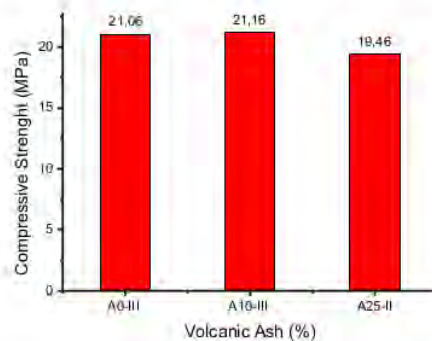


**FIGURE 3.2** Graph of compressive strength of concrete against variations in volcanic ash.

The compressive strength of concrete A<sub>0-I</sub>, A<sub>0-II</sub>, A<sub>0-III</sub> normal concrete (0%) with the quality of concrete K175 has compressive strengths are 20.35 MPa, 19.34 MPa, and 21.06 MPa, concrete A<sub>6-I</sub>, A<sub>6-II</sub>, A<sub>6-III</sub> has compressive strengths of 18.34 MPa, 19.80 MPa, 18.41 MPa, concrete A<sub>8-I</sub>, A<sub>8-II</sub>, A<sub>8-III</sub> have compressive strengths of 18.06 MPa, 17.94 MPa, 17.59 MPa, respectively. Concrete A<sub>10-I</sub>, A<sub>10-II</sub>

and A<sub>10-II</sub> are concrete with a mixture of volcanic ash of 10% having compressive strengths of 19.00 MPa, 19.38 MPa and 21.16 MPa, concrete A<sub>12-I</sub>, A<sub>12-II</sub>, A<sub>12-III</sub> (12%) has sequential compressive strengths of 17.88 MPa, 17.29 MPa and 17.75 MPa. Concrete K175 based on (density analysis) XRD volcanic ash mixture of 15%, 20%, 25% and 30%, has a compressive strength of concrete B<sub>15-I</sub>, B<sub>15-II</sub> are 16.15 MPa and 15.47 MPa, respectively. Concrete B<sub>20-I</sub> and B<sub>20-II</sub> have compressive strengths of 16.35 MPa and 15.41 MPa, concrete B<sub>25-I</sub> and B<sub>25-II</sub> with a mixture of volcanic ash respectively 25% compressive strength are 18.33 MPa and 19.46 MPa. Concrete B<sub>30-I</sub> and B<sub>30-II</sub> have compressive strengths of 18.06 MPa and 16.87 MPa. So the selected sample on K175 quality concrete is betton A<sub>0-III</sub> (0%) with compressive strength of 21.06 MPa, A<sub>10-III</sub> (10%) with compressive strength of 21.16 MPa and based on (density analysis) XRD is B<sub>25-II</sub> (25%) with a compressive strength of 19.46 MPa can be seen Figure 3.2.

### 3.3 Analysis of XRD Test Results

XRD testing is carried out to identify the phase in each concrete sample. Through this test obtained formed phases, and crystal structures. The data obtained were analyzed using Match v3.8.0 software. Below is the result of the diffraction pattern of K175 quality concrete with the addition of volcanic ash to A<sub>10-III</sub> and B<sub>25-II</sub>, while A<sub>0-III</sub> without the addition of volcanic ash.

Figure 3.3 shows the pattern of volcanic ash reactors (0%), showing the formation of SiO<sub>2</sub>, Ca(OH)<sub>2</sub>, CaCO<sub>3</sub> and optimum SiO<sub>2</sub> phases at an angle of  $2\theta = 26.73^\circ$  with an intensity of 804.3 (a.u) while Ca(OH)<sub>2</sub> phase is present in two the angle is  $2\theta = 18.12^\circ$ , and  $2\theta = 34.19^\circ$  with an intensity of 269 (au) and 286.4 (au) CaCO<sub>3</sub> phase at an angle of  $2\theta = 29.53^\circ$  with an intensity of 293.6 (a.u). The diffraction pattern (10%) of the phases formed are SiO<sub>2</sub>, Ca (OH)<sub>2</sub>, CaCO<sub>3</sub>, and NiSi<sub>2</sub>. The SiO<sub>2</sub> phase experiences a peak shift towards the left and is optimum at an angle of  $2\theta = 26.58^\circ$  with an intensity of 647.7 (a.u) while the Ca(OH)<sub>2</sub> phase is at an angle of  $2\theta = 34.1^\circ$  with an intensity of 237.1 (a.u). The CaCO<sub>3</sub> phase is at an angle of  $2\theta = 29.36^\circ$  with an intensity of 148.5 (a.u), in the NiSi<sub>2</sub> phase there is an angle of  $2\theta = 47.53^\circ$  with an intensity of 231.3 (a.u).

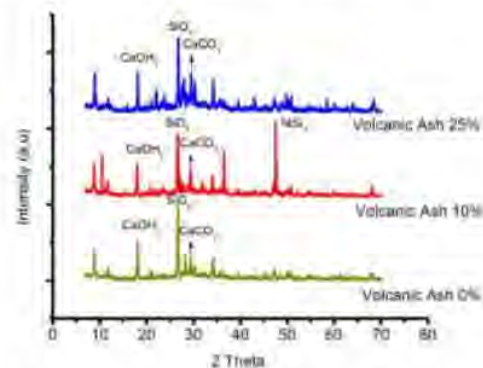


**FIGURE 3.3** Diffraction patterns of K175 quality concrete with the addition of volcanic ash A<sub>10-III</sub> and B<sub>25-II</sub>, without the addition of volcanic ash A<sub>0-III</sub>.

The diffraction pattern (25%) formed phases are SiO<sub>2</sub>, Ca(OH)<sub>2</sub> and CaCO<sub>3</sub>. The SiO<sub>2</sub> phase experiences a peak shift towards the left and is optimum at an angle of  $2\theta = 26.66^\circ$  with an intensity of 753.1 (a.u). The Ca(OH)<sub>2</sub> phases are at two angles  $2\theta = 18.06^\circ$  and  $2\theta = 34.11^\circ$  with intensities of 309.5 (a.u) and 498.4 (a.u), respectively. The CaCO<sub>3</sub> phase is at an angle of  $2\theta = 29.39^\circ$  with an intensity of 512.2 (a.u).

Based on Figure 3.3, it can be concluded that  $\text{SiO}_2$  has the greatest intensity compared to other elements contained in concrete. Crystal structure formed in K175 quality concrete without the addition of A0-III volcanic ash, the addition of A10-III and B25-II volcanic ash contained  $\text{SiO}_2$  supported by [17],  $\text{Ca}(\text{OH})_2$  and  $\text{CaCO}_3$  supported by [18]; [19], and there was an addition of  $\text{NiSi}_2$  to A<sub>10-III</sub> concrete with the addition of 10% volcanic ash.

The main compounds in cement are  $3\text{CaO} \cdot \{\text{SiO}_2\}$  labeled C3S in the chemical shorthand notation of cement  $2\text{CaO} \cdot \{\text{SiO}_2\}$  labeled C2S, and  $3\text{CaO} \cdot \{\text{Al}_2\text{O}_3\}$  labeled C3, and solid solutions with an average composition of  $4\text{CaO} \cdot \{\text{Al}_2\text{O}_3 \cdot \{\text{Fe}_2\text{O}_3\}\}$  labeled C4AF [8].

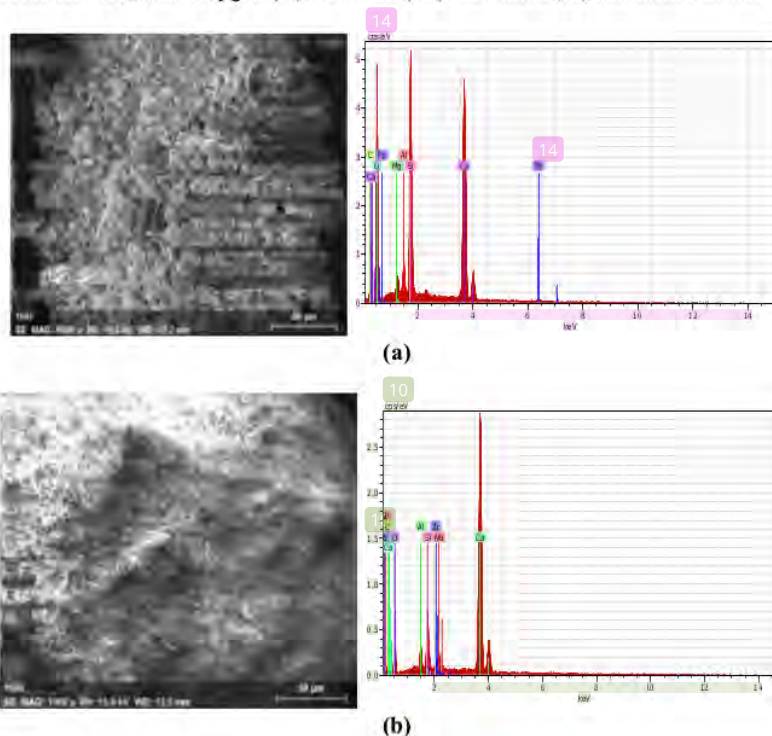
### 3.4 Analysis of SEM Test Results

The SEM test has been used by [8] to look at morphology, EDX [20]; [21] to find out the composition of K175 quality concrete compound using a mixture of volcanic ash. From SEM magnification 1000 times, the following picture SEM test results on concrete samples.

If the aggregate has finer grain size and varies in size, then the pore volume of the concrete becomes smaller. This is because smaller grains will fill the pores between the larger grains, so that the pores become smaller and concrete has high compressive strength and has a small porosity. Fine aggregates meet international organizational standards for standardization (ISO) that the  $\text{SiO}_2$  content is not less than 98% and the particle size ranges between 80  $\mu\text{m}$  and 2 mm [5], the largest pores to the smallest can be seen in Figure 3.4 (a), (c) and (b).

Based on research [19] portland cement with the addition of 3%  $\text{SiO}_2$  has a denser structure, finer and the content of  $\text{Ca}(\text{OH})_2$  decreases, in finer structures a higher compressive strength is formed.

After testing SEM-EDX K175 quality concrete according to SNI normal concrete A<sub>0-III</sub> has Oxygen (O), Calcium (Ca) and Silica (Si), A<sub>10-III</sub> concrete has Calcium (Ca), Oxygen (O) and Silica (Si) whereas in concrete B<sub>25-II</sub> has Oxygen (O), Calcium (Ca) and Silica (Si) can form CaO and SiO [8].



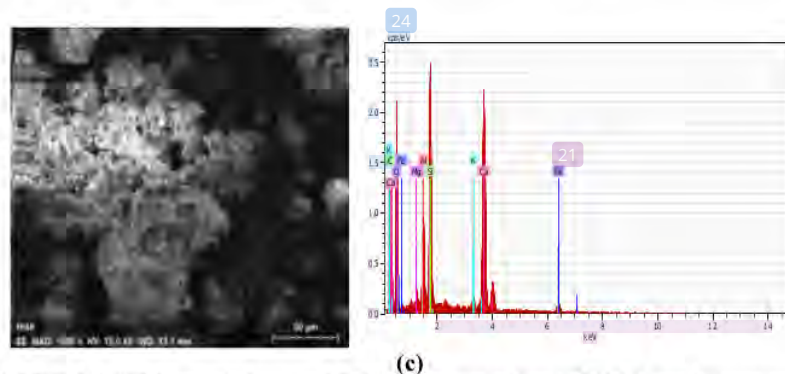


**FIGURE 3.4** SEM morphology and EDX characterization of K175 quality concrete (a) without  $A_{0-III}$  volcanic ash (b)  $A_{10-III}$  volcanic ash (c)  $B_{25-II}$  volcanic ash with 1000 times magnification.

**TABLE 2.3** Composition of compounds from SEM-EDX in concrete  $A_{0-III}$ ,  $A_{10-III}$  and  $B_{25-II}$

Chemical Element	Mass %	Chemical Element	Mass %	Chemical Element	Mass %
$A_{0-III}$		$A_{10-III}$		$B_{25-II}$	
O	49.68	O	31.38	O	45.67
Ca	30.03	Ca	54.62	Ca	28.85
Si	12.40	Si	4.46	Si	12.61
C	4.12	C	3.90	C	3.56
Al	1.69	Al	1.71	Al	4.09
Mg	1.09	Nb	2.94	Mg	0.63
Fe	0.98	Zr	0.99	Fe	2.94
				K	1.08

Based on table 2.3 there are elements of Si, Al, Fe and O, meaning concrete contains pozzolanic material ( $SiO_2$ ,  $Al_2O_3$ ,  $Fe_2O_3$ ) [4] as well as  $SiO_2$ ,  $CaCO_3$  concrete material [8], calcium silicate hydrate (CSH), portlandite ( $Ca(OH)_2$ ), oxidation of iron hydroxide ( $Fe(OH)_2$ ), decarbonation of calcium carbonate ( $CaCO_3$ ) discoloration on concrete surfaces related to oxidation and decarbonation reactions [16].

### 3.5 Analysis Fourier Infrared Spectroscopy (FTIR)

Characterization of concrete  $A_{0-III}$ ,  $A_{10-III}$  and  $B_{25-II}$  using FTIR in the wave range  $500-4000\text{ cm}^{-1}$ . The results of the test are shown in Figure 3.5 below.

The results of the FTIR functional group analysis showed that the addition of volcanic ash did not cause a new functional group in concrete, marked by the presence of a band that showed the Si-O-Si bond changed significantly. [1] volcanic ash has a wave number (wavenumber) between  $1200-2400\text{ cm}^{-1}$ , wave number at  $1004\text{ cm}^{-1}$  there is Si-O-Si, at  $1428\text{ cm}^{-1}$  there is O-C-O, at  $2358\text{ cm}^{-1}$  there are O-H and H-O-H. The FTIR spectra of Portland anhydrous cement [19] has a wave number at  $3570-3200\text{ cm}^{-1}$  with OH-OH, at  $3640\text{ cm}^{-1}$  there is  $Ca(OH)_2$ . FT-IR wave numbers at  $1300 - 1000$ ,  $807$ , and  $478\text{ cm}^{-1}$  were found in pure silica ( $SiO_2$ ) samples for asymmetrical, symmetrical, tissue and bending [22], wave numbers  $1947\text{ cm}^{-1}$  in Ni-Si samples [23]. The Transmittance% pattern of the wave numbers of concrete  $A_{0-III}$ ,  $A_{10-III}$  and  $A_{25-II}$  shown in Figure 3.5 produces the functional groups shown in Table 2.4.

FTIR test on normal concrete  $A_{0-III}$  above shows that there are two peaks at wave numbers  $874.67$  and  $987.81$ , which are special features of the SiO peak. The results of FTIR concrete with the addition of volcanic ash as much as 25% of the amount of sand appear one peak at wave number  $1000.82$ ,

while the concrete with the addition of volcanic ash as much as 10% of the amount of cement appear one peak at wave number 1003.3 which is a special feature of the peak of SiO. Wave numbers for SiO functional groups in variations A<sub>10-III</sub> and B<sub>25-III</sub> (with the addition of volcanic ash) there is a shift in the peak / sharper. This happens because of the addition of volcanic ash which causes changes in the vibrational frequency of the SiO<sub>2</sub> molecule. The peak wave number 3400 - 4000 cm<sup>-1</sup> shows the O - H bond which is a stretching and bending vibration, it is seen an increase in the sharpness of the absorption peak, [19] strengthen SiO<sub>2</sub> so that the compressive strength of concrete with a mixture of 10% high volcanic ash and small concrete pores by The SEM shown in Figure 3.4. Based on research conducted by [1] on Fly-ash obtained SiO<sub>2</sub> functional groups there are peaks at wave number 1004.10 cm<sup>-1</sup> and O-H function groups at wave numbers 3715 - 2358 cm<sup>-1</sup>.

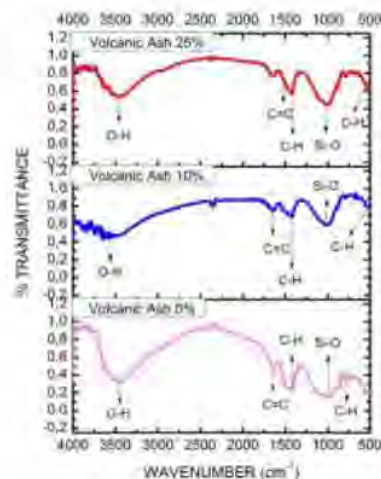


**FIGURE 3.5** FTIR Characterization of concrete functional groups A<sub>0-III</sub>, A<sub>10-III</sub> and A<sub>25-III</sub>.

**TABLE 2.4** Function clusters observed in FTIR testing [1].

Bonds	A <sub>0-III</sub> (cm <sup>-1</sup> )	A <sub>10-III</sub> (cm <sup>-1</sup> )	A <sub>25-III</sub> (cm <sup>-1</sup> )
Stretching vibration (OH, H-O-H)	3443.02 - 1650.77	3301-2333	3304-2343
Bending vibration (H-O-H)	-	1652	1653
Stretching vibration (C=O)	1650.77	-	-
Asymmetric stretching (Si-O-Si)	874.67, 987.81	970	969
Ni-Si	-	1974	-

FTIR test on normal concrete A0-III above shows that there are two peaks at wave numbers 874.67 and 987.81, which are special features of the SiO peak. The results of FTIR concrete with the addition of volcanic ash as much as 25% of the amount of sand appear one peak at wave number 1000.82, while the concrete with the addition of volcanic ash as much as 10% of the amount of cement appear one peak at wave number 1003.3 which is a special feature of the peak of SiO. Wave numbers for SiO functional groups in variations A<sub>10-III</sub> and B<sub>25-III</sub> (with the addition of volcanic ash) there is a shift in the peak / sharper as shown in Table 2.5. This happens because of the addition of volcanic ash which causes changes in the vibrational frequency of the SiO<sub>2</sub> molecule. The peak wave number 3400 - 4000

$\text{cm}^{-1}$  shows the O - H bond which is a stretching and bending vibration, it is seen an increase in the sharpness of the absorption peak, [19] strengthen  $\text{SiO}_2$  so that the compressive strength of concrete with a mixture of 10% high volcanic ash and small concrete pores by The SEM shown in Figure 3.4. Based on research conducted by [1] on Fly-ash obtained  $\text{SiO}_2$  functional groups there are peaks at wave number  $1004.10 \text{ cm}^{-1}$  and O-H function groups at wave numbers  $3715 - 2358 \text{ cm}^{-1}$ .

**Table 2.5** Function groups of K175 quality concrete using volcanic ash

Volcanic Ash %	Wavenumbers $\text{cm}^{-1}$		Functional Groups
	Quality Concrete K175	Frequency Area	
A <sub>0-III</sub>	779.16	675 – 900	C – H
	874.67, 987.81	1400 – 800	Si – O
	1417.21	1340 – 1470	C – H
	1650.77	1690-1760	C = O
	3443.02	3300-4000	O – H
A <sub>10-III</sub>	472.17	675 – 900	C – H
	1003.31	1400 – 800	Si – O
	1423.75, 1458.40	1340 – 1470	C – H
	1508.53, 1650.10	1500 – 1680	C = C
	3504.76, 3525.22,	3300 – 4000	O – H
	3546.60, 3567.07,		
3588.82, 3615.96,			
3945.53			
B <sub>25-II</sub>	467.84, 875.04	675 – 900	C – H
	1000.82	1400 – 800	Si – O
	1419.67,	1340 – 1470	C – H
	1493.18, 1510.98	1500 – 1680	C = C
	3435.90, 3572.60,	3300 – 4000	O – H
	3622.70, 3633.63,		
3655.39			

#### 4. Conclusion

Sifted volcanic ash added to K175 quality concrete acts as a substitute for cement for A<sub>10</sub> concrete and without sifting acts as an aggregate substitute for B<sub>25</sub> concrete, analyzed from absorption and compressive strength followed by characterization of XRD, SEM-EDX and FTIR. The following is the novelty obtained is the absorption is proportional to the compressive strength,  $\text{NiSi}_2$  can increase the compressive strength of concrete.

#### 5. Acknowledgments

This gratitude is addressed to Medan State University for providing Student Grant assistance to my thesis guidance students, as well as to the Ministry of Ritsek-Dikti in uploading a free international journal as a reference to registration at Simlitabmas.

#### 6. References

- [1] Abdullah, M. M. A. B., Hussin, K., Bnhussain, M., Ismail, K. N., Yahya, Z. and Razak, R. A., (2012), Fly Ash-based Geopolymer Lightweight Concrete Using Foaming Agent, *Int. J. Mol. Sci*, 13 : 7186-7198.
- [2] Abdullah, M. M. A. B., Hussin, K., Bnhussain, M., Ismail, K. N., Yahya, Z. and Razak, R. A.,

- (2012), Fly Ash-based Geopolymer Lightweight Concrete Using Foaming Agent, *Int. J. Mol. Sci.*, *13* : 7186-7198.
- [3] Kabir, H., and Sadeghi, M., (2017), Reactive Silica Sand Powder Concrete (RSSPC) Uniaxial Compressive Strength Investigation, *The Open Access Journal of Science and Technology* vol. 5 (2017), Article ID 101230, 8 pages.
- [4] Goracci, G., Monasterio M., Helen Jansson H. And Silvina Cerveny, S., (2017), Dynamics of nano-confined water in Portland cement – comparison with synthetic C-S-H gel and other silicate materials, *Scientific Reports* | *7*: 8258 |.
- [5] Liu, R., Liu, H., Sha, F., Yang, H., Zhang, Q., Shi, S. and Zheng, Z., (2018), Investigation of the Porosity Distribution, Permeability, and Mechanical Performance of Pervious Concretes, *Processes*, *6*, 78.
- [6] Kwon, Y. H., Kang, S. H., Hong, S. G. and Moon, J., (2017), Intensified Pozzolanic Reaction on Kaolinite Clay-Based Mortar, *Appl. Sci.*, *7*, 522.
- [7] Razak, R. A., Abdullah, M. A. B., Hussin, K., Ismail, K. N., Hardjito, D., 5 and Yahya, Z., (2015), *Int. J. Mol. Sci.*, *16* : 11629-11647.
- [8] Bravo, S., Parra, M. J., Castillo, R., Sepúlveda, F., Turner, A., Bertín, A., Osorio, G., Tereszczuk, J., Bruna, C. and Hasbún, R., (2016), Reversible *in vivo* cellular changes occur during desiccation and recovery: Desiccation tolerance of the resurrection filmy fern *Hymenophyllum dentatum* Cav, *Gayana Bot.* *73*(2), 402-413.
- [9] Guedes, M., Evangelista, L., Brito, J. D., and Ferro, A. C., (2013), Microstructural Characterization of Concrete Prepared with Recycled Aggregates, *Microsc. Microanal.* *19*, 1222–1230.
- [10] Hasan, H. W. U., Sabahat Alamgir, S., Ahmed, H., and Mubin, S., (2014), Experimental Investigation of Tensile and Flexural Strength of Ceramic Waste Concrete, *Pakistan Journal of Science* Vol. 66 No. 1 March.
- [11] Yanweerasak, T., Kea, T. M., Ishibash, H., and Akiyama, M., (2018), Effect of Recycled Aggregate Quality on the Bond Behavior and Shear Strength of RC Members, *Appl. Sci.*, *8*, 2054.
- [12] Yang, S., (2018) Effect of Different Types of Recycled Concrete Aggregates on Equivalent Concrete Strength and Drying Shrinkage Properties, *Appl. Sci.*, *8*, 2190.
- [13] Vural, B., (2011), Determination of Alkali-Silica Reaction in a Seismic Zone of The Turkey, *International Journal of Arts & Sciences*, *4*(19):53–60.
- [14] Montes, F., Valavala, S., and Haselbach, L. M., 2005, A New Test Method for Porosity Measurements of Portland Cement Pervious Concrete, *Journal of ASTM International*, January 2005, Vol. 2, No. 1 Paper ID JAI12931.
- [15] Siddiqi, Z. A., Hameed, R., Saleem, M., Khan, Q. S., and Ishaq, I., (2013), Performance Study of Locally Available Coarse Aggregates of Azad Kashmir, *Pakistan Journal of Science* (Vol. 65 No. 1 March).
- [16] Yanya, Y., (2018), Blending ratio of recycled aggregate on the performance of pervious concrete, *Y. Yanya, Frattura ed Integrità Strutturale*, *46* : 343-351.
- [17] Duan, Z., Hou, S., Poon, C. S., Xiao, J., and Liu, Y., (2018), Using Neural Networks to Determine the Significance of Aggregate Characteristics Affecting the Mechanical Properties of Recycled Aggregate Concrete, *Appl. Sci.*, *8*, 2171.
- [18] Alqassim, M.A., Jones, M.R., Berlouis, L.E.A., Daeid, N. N., (2016), A thermoanalytical, X-ray diffraction and petrographic approach to the forensic assessment of fire affected concrete in the United Arab Emirates. *Science International* *264* (2016) 82–88.
- [19] Voicu, G., Popa, A. M., Badanoiu, A. I., and Iordache, F., (2016), Influence of Thermal Treatment Conditions on the Properties of Dental Silicate Cements, *Molecules*, *21*, 233.
- [20] Wang, L., Zheng, D., Zhang, S., Cui, H. and Li, D., (2016), Effect of Nano-SiO<sub>2</sub> on the Hydration and Microstructure of Portland Cement, *Nanomaterials*, *6*, 241.
- [21] Mansur, A. A. P. and Mansur, H. S., (2009), Preparation and characterization of 3D porous

- ceramic scaffolds based on portland cement for bone tissue engineering, *J Mater Sci: Mater Med*, 20:497–505.
- [22] Alqedairi, A., Viveros, C. A. M., Pantera-Jr., E. A., Funollet, M. C., Alfawaz, H., Neel, E. A. A., and Abuhaimed, T. S., (2017), Superfast Set, Strong and Less Degradable Mineral Trioxide Aggregate Cement, Volume, Article ID 3019136, 9 pages.
- [23] Chan, Y. T., Kuan, W. H., Tzoul, Y. M., Chen, T. Y., Liu, Y. T., Wang, M. K., and Teah, H. Y., (2016), Molecular Structures of Al/Si and Fe/Si Coprecipitates and the Implication for Selenite Removal, *Scientific Reports* | 6:24716 |.
- [24] YAGI, T. and Higuchi, Y., (2013 ), Studies on hydrogenase, *Proc. Jpn. Acad., Ser. B* 89: 16-33.



# Characterization of K175 Concrete SNI Standards Using Volcanic Ash Aggregates With Variation in Composition

## ORIGINALITY REPORT

**21** %  
SIMILARITY INDEX

**15** %  
INTERNET SOURCES

**16** %  
PUBLICATIONS

**7** %  
STUDENT PAPERS

## PRIMARY SOURCES

- 1** Dwi Fany Butar-Butar, Efendi Napitupulu, Dina Ampera. "Development of E - Learning Based "SMILE" Learning Model to Improve Economic Learning Outcomes of Class X Students of Senior High School 1 Pahae Jae 2019/2020", *Journal of Physics: Conference Series*, 2020  
Publication **3** %
- 2** [www.ncbi.nlm.nih.gov](http://www.ncbi.nlm.nih.gov)  
Internet Source **2** %
- 3** [www.kenzpub.com](http://www.kenzpub.com)  
Internet Source **2** %
- 4** R D Susanti, R B Abdulrajak, J Gowasa, D I Siahaan. "Potential mixture cold lava sand and volcanic ash as a concrete admixture", *IOP Conference Series: Materials Science and Engineering*, 2021  
Publication **1** %
- 5** Submitted to Higher Education Commission Pakistan  
Student Paper **1** %

6	<a href="http://www.mdpi.com">www.mdpi.com</a> Internet Source	1 %
7	<a href="http://www.nature.com">www.nature.com</a> Internet Source	1 %
8	<a href="http://eprints.whiterose.ac.uk">eprints.whiterose.ac.uk</a> Internet Source	1 %
9	Mafalda Guedes, Luís Evangelista, Jorge de Brito, Alberto C. Ferro. "Microstructural Characterization of Concrete Prepared with Recycled Aggregates", Microscopy and Microanalysis, 2013 Publication	1 %
10	Submitted to Universiti Tenaga Nasional Student Paper	<1 %
11	Submitted to Padjadjaran University Student Paper	<1 %
12	Wan Mastura Wan Ibrahim, Mohd Mustafa Al Bakri Abdullah, Romisuhani Ahmad, Muhammad Faheem Mohd Tahir et al. "Mechanical and physical properties of bottom ash/fly ash geopolymers for pavement brick application", IOP Conference Series: Materials Science and Engineering, 2020 Publication	<1 %
13	<a href="http://www.cambridge.org">www.cambridge.org</a> Internet Source	<1 %

14	<a href="http://academicrepository.khas.edu.tr">academicrepository.khas.edu.tr</a> Internet Source	<1 %
15	"Preface", Journal of Physics: Conference Series, 2020 Publication	<1 %
16	Submitted to Universiti Malaysia Kelantan Student Paper	<1 %
17	<a href="http://ips.pps.unm.ac.id">ips.pps.unm.ac.id</a> Internet Source	<1 %
18	<a href="http://Digilib.Unimed.Ac.Id">Digilib.Unimed.Ac.Id</a> Internet Source	<1 %
19	<a href="http://basharesearch.com">basharesearch.com</a> Internet Source	<1 %
20	<a href="http://semenpadang.co.id">semenpadang.co.id</a> Internet Source	<1 %
21	Submitted to National Institute of Technology, Hamirpur Student Paper	<1 %
22	<a href="http://discovery.dundee.ac.uk">discovery.dundee.ac.uk</a> Internet Source	<1 %
23	Ya-Ting Chan, Wen-Hui Kuan, Yu-Min Tzou, Tsan-Yao Chen, Yu-Ting Liu, Ming-Kuang Wang, Heng-Yi Teah. "Molecular Structures of Al/Si and Fe/Si Coprecipitates and the	<1 %

# Implication for Selenite Removal", Scientific Reports, 2016

Publication

---

24	<a href="http://doczz.net">doczz.net</a> Internet Source	<1 %
25	<a href="http://sinta3.ristekdikti.go.id">sinta3.ristekdikti.go.id</a> Internet Source	<1 %
26	<a href="http://www.zag.si">www.zag.si</a> Internet Source	<1 %
27	Submitted to Brewster High School Student Paper	<1 %
28	S. Bright Singh, M. Murugan. "Effect of aggregate size on properties of polypropylene and glass fibre-reinforced pervious concrete", International Journal of Pavement Engineering, 2020 Publication	<1 %
29	<a href="http://yayanindrapratamasewui.wordpress.com">yayanindrapratamasewui.wordpress.com</a> Internet Source	<1 %
30	<a href="http://ikm.za.pl">ikm.za.pl</a> Internet Source	<1 %
31	<a href="http://vdocuments.mx">vdocuments.mx</a> Internet Source	<1 %
32	<a href="http://www.fao.org">www.fao.org</a> Internet Source	<1 %

---

33

Tangchirapat, W.. "Use of waste ash from palm oil industry in concrete", Waste Management, 2007

Publication

<1 %

34

Tarek Uddin Mohammed, Aziz Hasan Mahmood, Shibly Mostafiz Apurbo, Munaz Ahmed Noor. "Substituting brick aggregate with induction furnace slag for sustainable concrete", Sustainable Materials and Technologies, 2021

Publication

<1 %

35

Wenchao Liu, Wanlin Cao, Nana Zong, Ruwei Wang, Lele Ren. "Experimental Study on Punching Performance of Recycled Aggregate Concrete Thin Wallboard with Single-Layer Reinforcement", Applied Sciences, 2018

Publication

<1 %

36

Zarina Yahya, Mohd Mustafa Al Bakri Abdullah, Leow Yee Jing, Long-Yuan Li, Rafiza Abd Razak. "Seawater Exposure Effect on Fly Ash based Geopolymer Concrete with Inclusion of Steel Fiber", IOP Conference Series: Materials Science and Engineering, 2020

Publication

<1 %

37

[acikerisim.dicle.edu.tr:8080](http://acikerisim.dicle.edu.tr:8080)

Internet Source

<1 %

38	<a href="http://journal.uet.edu.pk">journal.uet.edu.pk</a> Internet Source	<1 %
39	<a href="http://rasayanjournal.co.in">rasayanjournal.co.in</a> Internet Source	<1 %
40	<a href="http://res.mdpi.com">res.mdpi.com</a> Internet Source	<1 %
41	Mutiara Indah Sari, Syafruddin Ilyas, Tri Widyawati, Maya Anjelir Antika. " Effect of (linn) leaves ethanolic extract on blood glucose and malondialdehyde level in alloxan-induced diabetic rats ", IOP Conference Series: Earth and Environmental Science, 2018 Publication	<1 %
42	V.S. Babu, A.K. Mullick, K.K. Jain, P.K. Singh. "Strength and durability characteristics of high-strength concrete with recycled aggregate-influence of processing", Journal of Sustainable Cement-Based Materials, 2014 Publication	<1 %
43	<a href="http://elea.unisa.it">elea.unisa.it</a> Internet Source	<1 %
44	<a href="http://eprints.utm.my">eprints.utm.my</a> Internet Source	<1 %
45	<a href="http://upcommons.upc.edu">upcommons.upc.edu</a> Internet Source	<1 %

46

Internet Source

&lt;1 %

47

Kirthika S.K., S.K. Singh, Ajay Chourasia.  
"Alternative fine aggregates in production of sustainable concrete- A review", Journal of Cleaner Production, 2020

Publication

&lt;1 %

48

Miguel Bravo, António Santos Silva, Jorge de Brito, Luís Evangelista. "Microstructure of Concrete with Aggregates from Construction and Demolition Waste Recycling Plants", Microscopy and Microanalysis, 2015

Publication

&lt;1 %

49

Abdullah, Mohd Mustafa Al Bakri, Kamarudin Hussin, Mohamed Bnhussain, Khairul Nizar Ismail, Zarina Yahya, and Rafiza Abdul Razak. "Fly Ash-based Geopolymer Lightweight Concrete Using Foaming Agent", International Journal of Molecular Sciences, 2012.

Publication

&lt;1 %

50

Guido Goracci, Manuel Monasterio, Helen Jansson, Silvina Cervený. "Dynamics of nano-confined water in Portland cement - comparison with synthetic C-S-H gel and other silicate materials", Scientific Reports, 2017

Publication

&lt;1 %

51

M. Chakradhara Rao, Sriman Kumar  
Bhattacharyya, Sudhirkumar V. Barai.  
"Chapter 4 Properties of Recycled Aggregate  
Concrete", Springer Science and Business  
Media LLC, 2019

Publication

<1 %

52

Sungchul Yang. "Effect of Different Types of  
Recycled Concrete Aggregates on Equivalent  
Concrete Strength and Drying Shrinkage  
Properties", Applied Sciences, 2018

Publication

<1 %

53

Submitted to Far Eastern University

Student Paper

<1 %

Exclude quotes Off

Exclude matches Off

Exclude bibliography On



# Characterization of K175 Concrete SNI Standards Using Volcanic Ash Aggregates With Variation in Composition

---

GRADEMARK REPORT

---

FINAL GRADE

**/0**

GENERAL COMMENTS

**Instructor**

---

PAGE 1

---

PAGE 2

---

PAGE 3

---

PAGE 4

---

PAGE 5

---

PAGE 6

---

PAGE 7

---

PAGE 8

---

PAGE 9

---

PAGE 10

---

PAGE 11

---

PAGE 12

---

PAGE 13

---

PAGE 14

---

PAGE 15

---